

Quantification of Depth-Dependent Shear Strain Parameters at Varying Initial Shear Strains in Articular Cartilage

Chandler Woo (Class of 2017), Mark Buckley, Ph.D.

I. Abstract

Articular cartilage exhibits depth-dependent shear strain parameters due to its inhomogeneous composition. To better understand its mechanisms, adult human articular cartilage was examined to determine the effect depth of the cartilage has on local shear strain and phase angle when sheared at different strains (0% and 6%). Using confocal microscopy, photobleached lines were spaced evenly along the cartilage sample to track the displacement of the lines as functions of depth and time. Displacement is important in determining shear strain parameters because amplitude and phase shift can be extracted from an optimized fit of the sinusoidal response to derive local shear strain and phase angle for each depth z . Once these parameters are collected for each sample at each strain condition, a two-way ANOVA test can be conducted to determine the significance between shear strain parameters at specific depth ranges.

II. Introduction

The ability to facilitate the smooth motion between adjoining bone segments is possible through a class of flexible connective tissue called articular cartilage [1]. Composed of cells called chondrocytes surrounded by a matrix, articular cartilage tissue is approximately 70% to 85% water by weight with the remainder being composed of proteoglycans and collagen. Proteoglycan concentration and water content vary by depth of the tissue, with relatively low proteoglycan concentration while water content is highest at the articular surface [1]. Though articular cartilage performs several mechanical functions such as low friction and wear at joint locations, it is also known to have a set of quantifiable shear strain parameters that vary with depth. Distinguishing the differences between these depth-dependent parameters offers insight into how the inhomogeneous nature of articular cartilage can lead to its physiological function [2,3].

To better understand the depth-dependence of articular cartilage in relation to its local shear strain parameters, adult human articular cartilage samples were extracted [2,3]. Each sample was sheared sinusoidally at 1 Hz frequency under two different conditions: 0% initial strain applied ($n=4$) and 6% initial strain applied ($n=4$). To determine the effects of the two conditions, the cartilage samples were imaged using a confocal microscope. After positioning the samples, photobleached lines were spaced apart by 50 μm along the z -axis of the hemi-cylinder. Images were compiled and then analyzed to extract photobleached line locations in order to quantify local shear strain and phase angle for each sample at each condition. In order to determine whether shear strain parameters are significantly different as a result of depth, shear strain and phase angle for each sample are averaged at depths less than or equal to 250 μm and depths greater than 250 μm . Using numerical optimization to gather and analyze the data, shear strain and phase angle would be expected to be higher near

the articular surface as opposed to deeper in the tissue, exhibiting a global minimum near the surface of articular cartilage before plateauing at larger depths.

III. Experimental Data

Working in collaboration with Dr. Mark Buckley, 6 mm diameter cylindrical explants of 2-4 mm thicknesses were harvested from frozen adult human tibial plateaus [2]. Upon dissection, samples were bisected to hemi-cylinders and thawed in phosphate-buffered saline (PBS) solution for mechanical testing. Cartilage hemi-cylinders were set between two glass shearing plates of a tissue deformation imaging state (TDIS), with one face adhered to a stationary plate. Images were taken on an inverted Zeiss LSM 510 confocal microscope, observing the photobleached lines spaced 50 μm apart along the z -axis [2]. Articular cartilage data was collected in the form of confocal microscopic images at a frame rate of 100 fps. Each sample were sheared under two different conditions, 0% initial shear strain and 6% shear strain. Four samples were imaged for each initial shear strain condition, resulting in series of 200 confocal microscopic images of explanted cartilage sheared sinusoidally at 1 Hz frequency. The acquired images were analyzed to quantify local shear strain and phase angle of each sample.

IV. Data Analysis Methods

Visualization of the Data

Animations were constructed using 200 confocal microscopic images for each data set at a frame rate of 100 fps. A visual representation is described below (**Figure 1**), and full animations can be viewed in MATLAB.

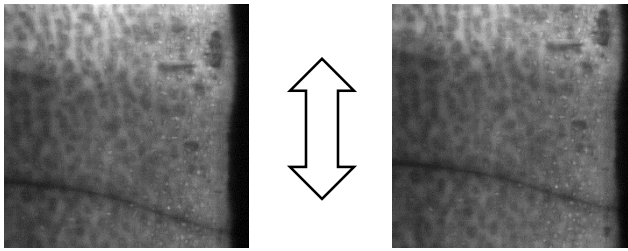


Figure 1. Visual representation of confocal images. Photobleached lines are characterized as dark lines in the images. Animations depict visible sinusoidal shifts in the z direction over time, as represented by the arrow.

Quantification of Shear Strain Parameters

A major component in quantifying the local shear strain and phase angle of the sample is the extraction of the photobleached line locations. By tracking the location of the photobleached lines, the sample displacement $u(z, t)$ relative to the undeformed state can be determined. The location of the photobleached lines can be extrapolated by isolating the local minima of the fluorescence intensity $I(x)$ profiles with respect to varying displacement x at a particular depth z . Noise along each displacement x can be minimized by fitting a parabola to ± 5 points around the local minimum in order to determine an initial guess. When this procedure is repeated for all 200 confocal images, $u(z, t)$ can be constructed [2,3].

Since the data is sheared sinusoidally, an unconstrained nonlinear optimization function can be applied to derive a best fit cosine function, $u(t) = u_0 \cos(\omega t + \delta_u)$, that extracts the amplitude u_0 and phase shift δ_u .

for each depth z . This nonlinear optimization function utilizes a standard procedure of sum of squared errors in order to optimize values for each input. These values can be then used to derive the local shear strain and phase angle for each depth z as described below:

$$\gamma_0(z) = \sqrt{\left[\frac{d}{dh}(u_0 \cos \delta_u)\right]^2 + \left[\frac{d}{dh}(u_0 \sin \delta_u)\right]^2} \quad (1)$$

$$\delta_\gamma(z) = \tan^{-1}\left[\frac{d}{dh}(u_0 \sin \delta_u) / \frac{d}{dh}(u_0 \cos \delta_u)\right] \quad (2)$$

where $h = L_0 - z$ and L_0 is the thickness of the sample. The numerical derivative is taken using a five-point linear least squares fitting (5PLSQ) technique with a polynomial curve fit of a first-order function, evaluating the slope of the adjacent two points on both sides of the data point in order to improve the derivative estimation (**Figure 2**).

Statistical Analysis

After determining the shear strain and phase angle at each depth z for each sample, statistical analysis is required to determine the 95% significance between the average $\gamma_0(z)$ and $\delta_\gamma(z)$ for $z \leq 250 \mu\text{m}$ and $z > 250 \mu\text{m}$. Since the data compares the difference in shear strain and phase angles at 0% shear and 6% shear, a two-way ANOVA calculation will determine the variance between the percent shear at two different depth regions. The two null hypotheses of the two-way ANOVA test assert that defined depth regions and initial percent shear do not affect shear strain or phase angle, respectively, and the alternative hypothesis being that either depth, initial percent shear, or both have a significant effect.

V. Results

Quantification of Shear Strain Parameters

In order to track a photobleached line, the local minima representing each line must be extracted. From each minimum at a specific depth z , a parabolic fit was established in order to set an initial guess to track the displacement as a function of depth and time (**Figure 3**). In the figures presented below, Sample 1 at 0% initial shear strain are presented to demonstrate the process of extracting local shear strain and phase angle values.

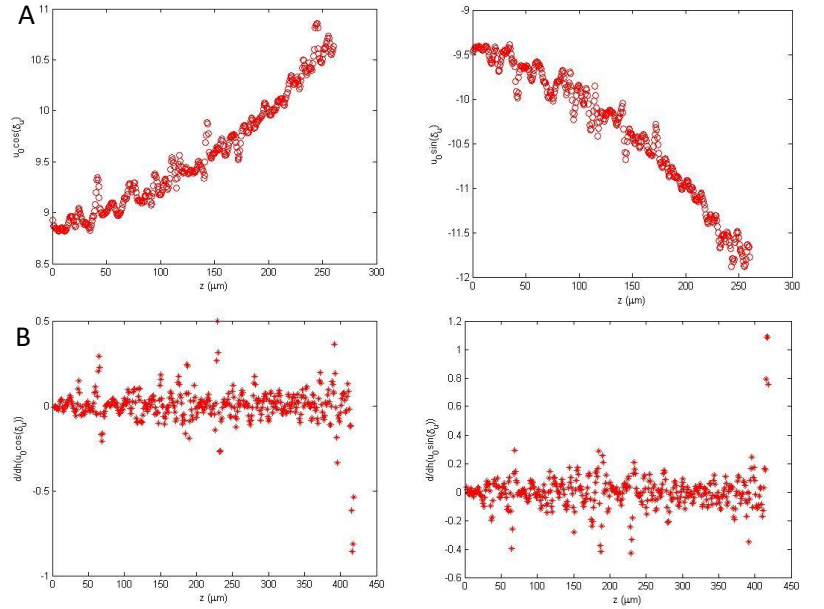


Figure 2. (A) Extracted cosine and sine plots, respectively, in terms of depth z using amplitude u_0 and phase δ_u from fits of $u(z,t)$. (B) Differentiated $u_0 \cos \delta_u$ and $u_0 \sin \delta_u$ plots, respectively, with respect to $h = L_0 - z$, using 5PLSQ.

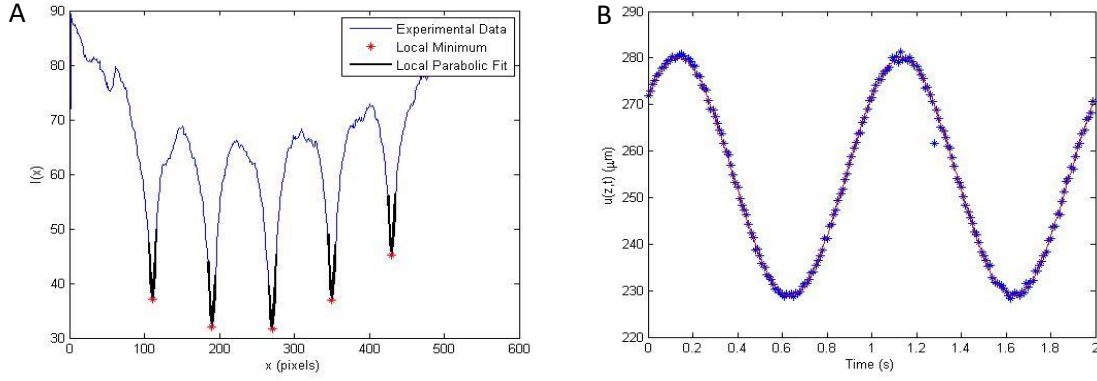


Figure 3. (A) Fluorescence intensity $I(x)$ at depth z for a sheared sample of articular cartilage at time t . Local parabolic fit near each line. (B) Mean $u(z,t)$ at depth z vs. time t . Red line depicts sinusoidal fit to data.

With the extracted, optimized sinusoid fit, cosine and sine functions can be derived as a function of depth, which is used to extract $\gamma_0(z)$ and $\delta_\gamma(z)$ from the data, as described below (**Figure 4**). These figures track the local shear strain amplitude and phase angle of Sample 1 and 0% initial strain. These values can be evaluated to determine whether there is significant statistical difference between 0% and 6% initial shear strain for varying depths.

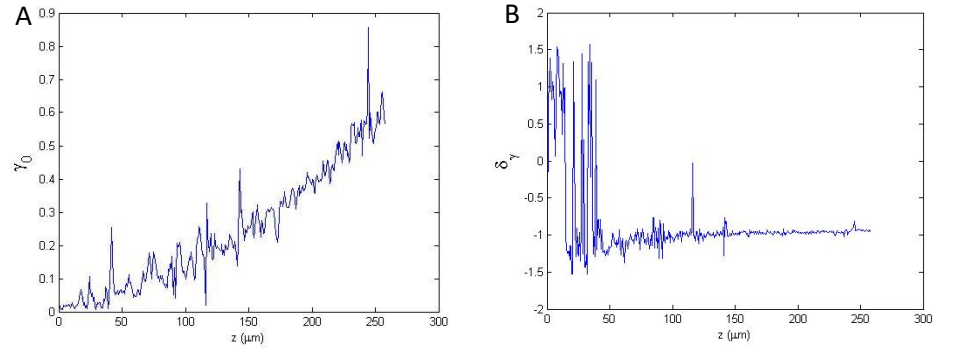
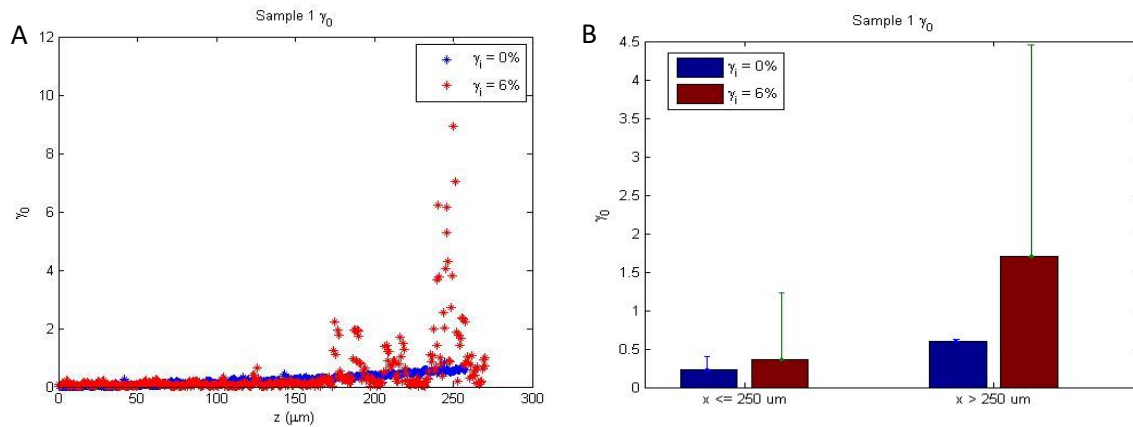


Figure 4. (A) Local shear strain amplitude γ_0 represented graphically as a function of z . (B) Local phase angle δ_γ represented graphically as a function of z .

Statistical Analysis

$\gamma_0(z)$ and $\delta_\gamma(z)$ are averaged for $z \leq 250 \mu\text{m}$ and for $z > 250 \mu\text{m}$ for each sample at each initial strain condition ($\gamma_i = 0$ and 6%) to observe differences at varying depths. Both initial strain conditions for each sample are analyzed to examine the effect of shear strain offset on the dynamic properties of articular cartilage (**Figure 5**). Figures of all samples can be found under Appendix C.



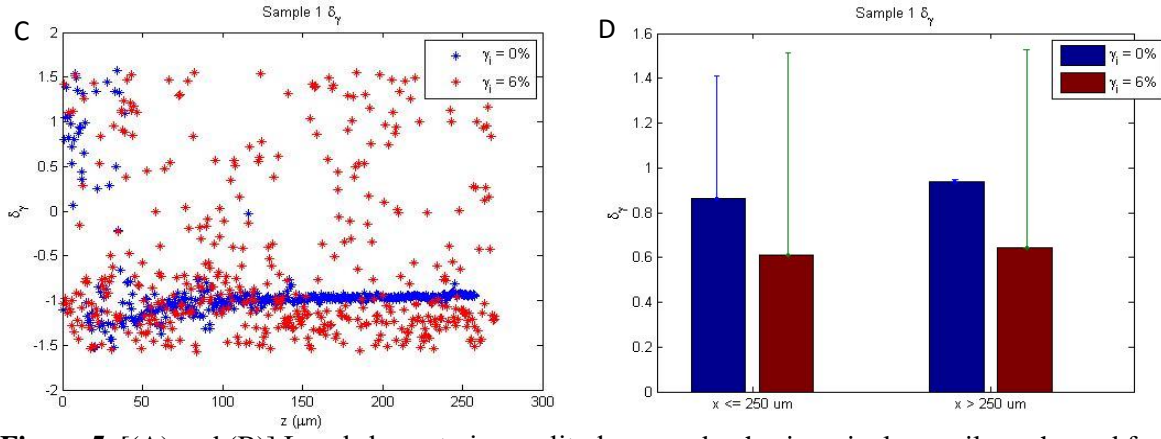


Figure 5. [(A) and (B)] Local shear strain amplitude γ_0 vs. depth z in articular cartilage sheared from initial strains ($\gamma_i = 0$ and 6%) with $f = 1$ Hz. Data are mean \pm SD, as indicated by error bars. [(C) and (D)] Phase angle δ_γ vs. depth z , following same process as shear strain amplitude.

Two-way ANOVA was conducted to determine if there is statistical significance between initial shear strains and depth-dependent parameters between all samples (Table 1, Table 2). From the tables, the reported p-values for initial shear strain condition (columns), depth (rows), and the interaction between the two for local shear strain amplitude γ_0 are $p = 0.1665$, $p = 0.0138$, and $p = 0.3205$, respectively. At a confidence of 95% ($\alpha = 0.05$), this suggests that while shear strain amplitude is significantly different between to depth locations, there is a large interaction between initial shear strain and depth that makes this test difficult to interpret. For phase angle, the p-values are $p = 0.4985$, $p = 0.6214$, and $p = 0.7427$, respectively, indicating that the interaction term is too large to interpret the model, possibly due to the presence of noise in the data.

ANOVA Table					
Source	SS	df	MS	F	Prob>F
Columns	0.21581	1	0.21581	2.17	0.1665
Rows	0.82616	1	0.82616	8.3	0.0138
Interaction	0.10682	1	0.10682	1.07	0.3205
Error	1.19384	12	0.09949		
Total	2.34263	15			

Table 1. Two-way ANOVA table for shear strain amplitude γ_0 .

ANOVA Table					
Source	SS	df	MS	F	Prob>F
Columns	0.28674	1	0.28674	0.49	0.4985
Rows	0.15123	1	0.15123	0.26	0.6214
Interaction	0.06645	1	0.06645	0.11	0.7427
Error	7.06404	12	0.58867		
Total	7.56845	15			

Table 2. Two-way ANOVA table for phase angle δ_γ .

VI. Discussion

In this study, image analysis was used to measure the depth-dependent shear strain parameters of adult human articular cartilage of varying initial applied shear strains. Given sets of confocal images for four different samples sheared at 0% and 6% initial strains, photobleached line locations were extracted from the minima of the intensity profile and tracked to model the displacement of the sample as it was sheared sinusoidally at a frequency of 1 Hz. In order to minimize noise present in the experiment, a parabola was fit using at least 20 points on both sides of the minima to smooth the response. Using 5PLSQ and optimization techniques, local shear strain amplitude and phase angle were determined from the amplitude and phase shift of the displacement profile. From the scatterplots described by Figure 5 and those under Appendix C, samples 2 and 4 present clear trends between 0% and 6% initial shear

strain that describe the expected response of the depth-dependent shear strain parameters. Local shear strain amplitude increased exponentially as it moved closer to the articular surface, with larger initial shear strains promoting larger amplitudes. On the other hand, phase angle appeared higher at larger initial shear strains but did not present an effect due to depth, as seen by the stable phase angle in Figure A under Appendix C. While these specific samples agree with our expectations that initial shear strain and depth play a role in articular cartilage mechanical properties, statistical significance was performed to confirm.

A two-way ANOVA test was conducted to determine if depth and initial shear strain exhibited effects on both local shear strain amplitude and phase angle. Analysis of the four samples yielded values as seen under **Appendix B**, and as described by **Tables 1** and **2**, the interaction term was large enough to make the model difficult to interpret. While statistical significance of cartilage depth was established for local shear strain amplitude, noise and error seen from samples 1 and 3 skewed the analysis and produced large interaction terms that ultimately indicated that no conclusion could be drawn for either local shear strain amplitude or phase angle. The noise in samples 1 and 3 presented significant outliers which is a product of the image analysis techniques used to extract the location of the photobleached lines. Choosing a minimum intensity value to find the location of a line could have been affected by the presence of stained proteoglycans, which may have stained darker than the photobleached line at that specific depth z and produced outliers along the sinusoidal curve. Future analysis should focus on deeper staining for the photobleached lines as well as stronger computational techniques to isolate the photobleached line, possibly through thresholding.

VII. Conclusion

This experiment tracked the displacement of articular cartilage as a function of time and depth in order to extract depth-dependent shear strain parameters at varying initial shear strain conditions. Through a series of image processing techniques, it was found that there is not a statistical significant difference between depths $z \leq 250 \mu\text{m}$ and $z > 250 \mu\text{m}$ for both local shear strain amplitude and phase angle. A significant difference was found between depths for local shear strain amplitude, but the large interaction between depth and initial shear strain makes it difficult to conclude definitively. This analysis may indicate that there are more factors such as viscoelastic properties and proteoglycan composition that must be considered when analyzing the inhomogeneous nature of articular cartilage tissue. A significant issue surrounding the study of articular cartilage is understanding the coordination between the mechanical and shear strain properties of articular cartilage that gives rise to its physiological functions. Once a stronger working model of the inhomogeneous nature of articular cartilage is known, further exploration of the function of tissue and other physiological systems can be developed.

VIII. Acknowledgments

I would like to thank Dr. Mark Buckley and his laboratory at the Department of Biomedical Engineering at University of Rochester for providing confocal microscopic images of sheared articular cartilage used in this report. Additionally, I would like to thank Dr. Regine Choe for assisting and evaluating the development of the project code as well as the formulation of this final report. Lastly, I would like to acknowledge my fellow students in BME 221 for collaborating and critiquing my analytical methods to improve its functionality.

IX. References

- [1] Mansour, Joseph M., Ph.D. “12 Biomechanics of Cartilage.” *Experimental Research Methods in Orthopedics and Trauma* (2015): 66-79. Web.
- [2] M R Buckley, A J Bergou, J Fouchard, L J Bonassar, and I Cohen. High-resolution spatial mapping of shear properties in cartilage. *J. Biomech.*, 43:796–800, 2010.
- [3] M R Buckley, L J Bonassar, and I Cohen. Localization of viscous behavior and shear energy dissipation in articular cartilage under dynamic shear loading. *J. Biomech. Eng.*, 135:31002, 2013.

X. Appendix

Appendix A: MATLAB Code List

Name	Functionality	Comments
part1.m	Main file 1	For section 1.2 – visualization of data
<i>video.m</i>	<i>Animation function</i>	<i>Compiles images into videos</i>
part2.m	Main file 2	For section 2.1 and 2.2 – find γ_0 and δ_γ
<i>avg_int.m</i>	<i>Intensity Profile function – 5 lines</i>	<i>Creates Figure 3(A) graphs</i>
<i>avg_int3.m</i>	<i>Intensity Profile function – 1 line</i>	<i>Models Fig 3(A) for 1 line</i>
<i>avg_disp.m</i>	<i>Line location function – 5 lines</i>	<i>Determine line location to develop Fig 3(B)</i>
<i>avg_disp3.m</i>	<i>Line location function z – 1 line</i>	<i>Models Fig 3(B) for 1 line</i>
<i>xpixel.m</i>	<i>x pixel length function</i>	<i>Determines x length based on samples</i>
<i>optimization.m</i>	<i>SSE function</i>	<i>Find SSE for best fine line of sinusoid</i>
stats.m	Main file 3	For section 3 – depth average and ANOVA

Appendix B: Extracted Data for Statistical Analysis

	$\gamma_i = 0\%$	$\gamma_i = 6\%$
mean($\gamma_0 \leq 250\ \mu\text{m}$)	0.2304	0.3630
	0.1412	0.2304
	0.0920	0.1177
	0.0618	0.0897
mean($\gamma_0 > 250\ \mu\text{m}$)	0.5958	1.7026
	0.4065	0.6926
	0.3202	0.4162
	0.3670	0.4609

	$\gamma_i = 0\%$	$\gamma_i = 6\%$
mean($\delta_\gamma \leq 250\ \mu\text{m}$)	-0.8624	-0.6126
	-0.7241	-0.4683
	-0.4595	-0.1765
	0.0867	0.8847
mean($\delta_\gamma > 250\ \mu\text{m}$)	-0.9392	-0.6418
	-0.8647	-0.4501
	1.1768	-0.2726
	-0.0389	1.2539

Appendix C: Additional Figures and Tables

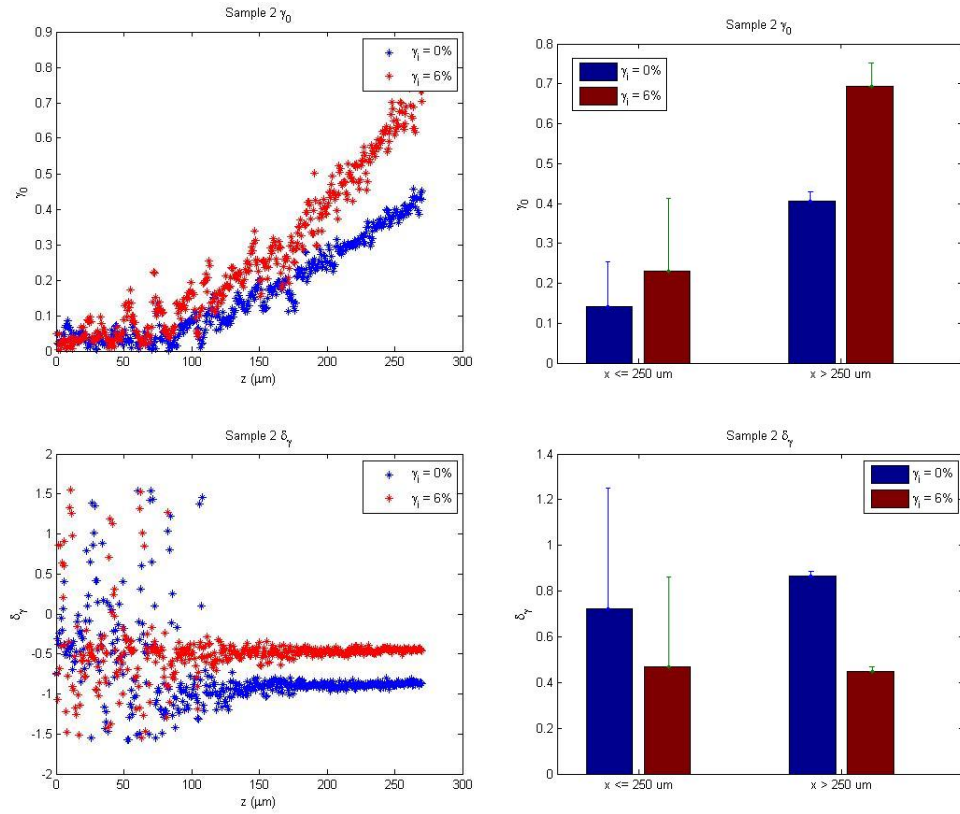


Figure A. Sample 2 local shear strain amplitude γ_0 vs. depth z in articular cartilage sheared from initial strains ($\gamma_i = 0$ and 6%) with $f = 1$ Hz. Data are mean \pm SD, as indicated by error bars. Phase angle δ_γ vs. depth z follows same process as shear strain amplitude.

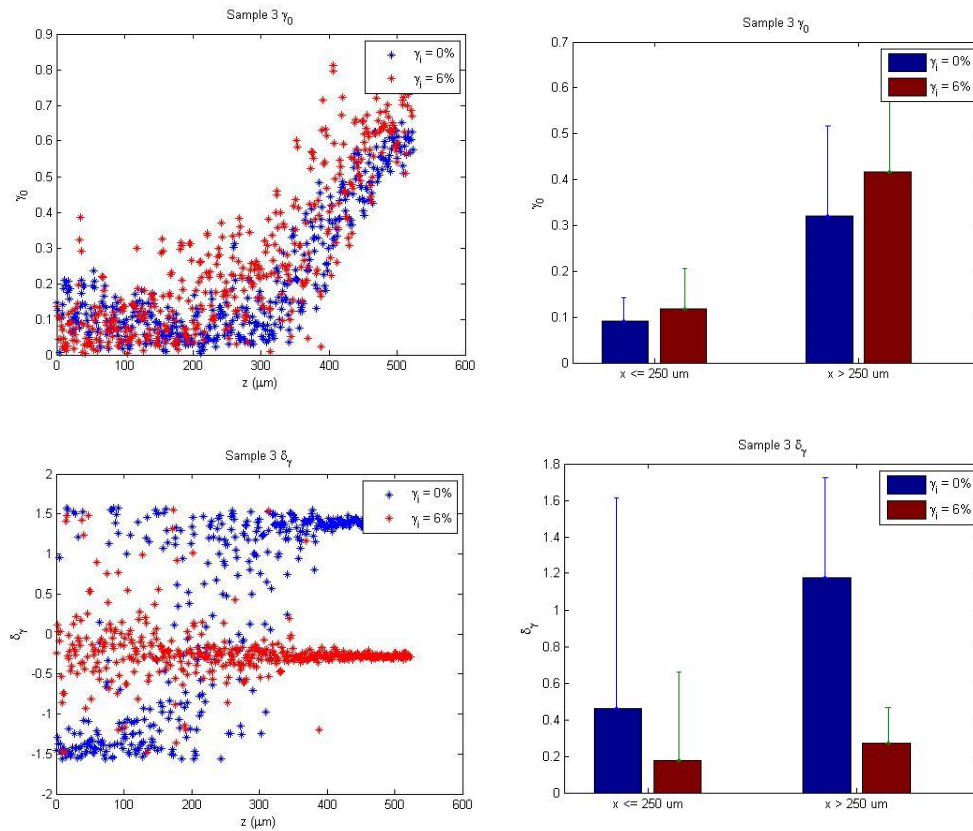


Figure B. Sample 3 local shear strain amplitude γ_0 vs. depth z in articular cartilage sheared from initial strains ($\gamma_i = 0$ and 6%) with $f = 1$ Hz. Data are mean \pm SD, as indicated by error bars. Phase angle δ_γ vs. depth z follows same process as shear strain amplitude.

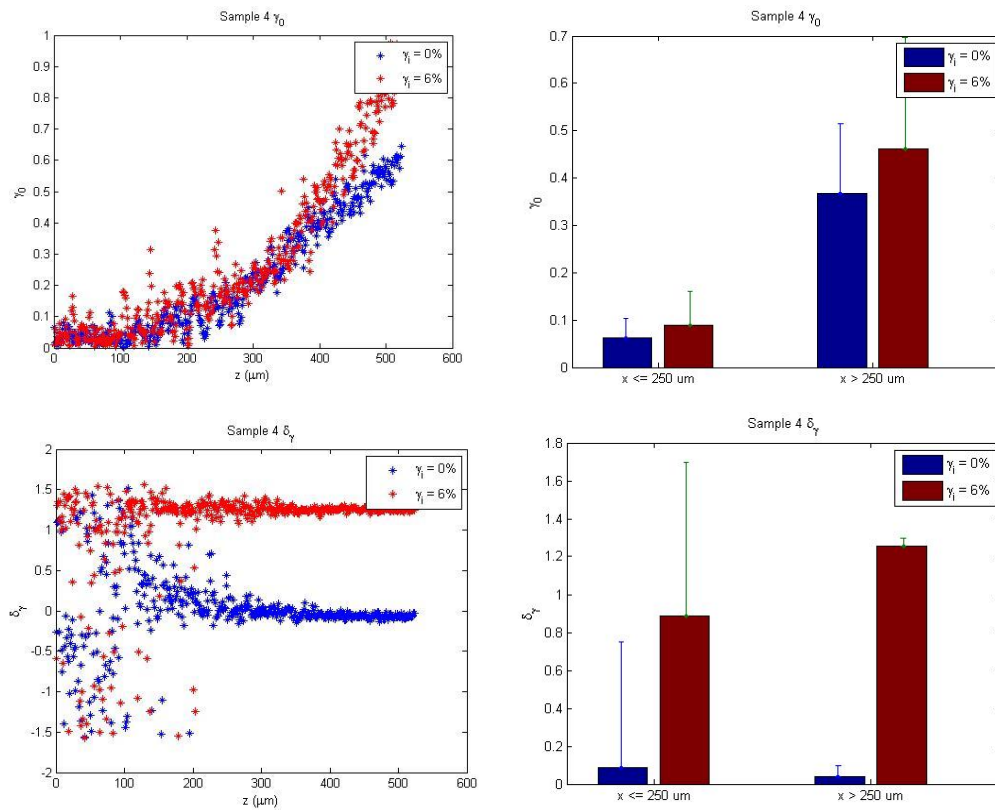


Figure C. Sample 4 local shear strain amplitude γ_0 vs. depth z in articular cartilage sheared from initial strains ($\gamma_i = 0$ and 6%) with $f = 1$ Hz. Data are mean \pm SD, as indicated by error bars. Phase angle δ_γ vs. depth z follows same process as shear strain amplitude.

Appendix D: Extra Credit

N/A

Appendix E: Disclaimer

This document is a part of BME 221 final project requirement, simulating the writing process for a peer-reviewed manuscript. Professor Mark Buckley provided the original data that this project was based on. More details about the data can be found in the References section [2,3].